Flow Distribution Analysis of the Solid Oxide Fuel Cell Stack under Electric Load Conditions

Janusz Jewulski, Marcin Blesznowski, Michal Stepien
Institute of Power Engineering
ul. Augustowka 36
PL-02-981 Warszawa / Poland
Tel.: +48-22-345-1410,
Fax: +48-22-642-8378
janusz.jewulski@ien.com.pl

Abstract

The flow distribution of reactants is one of the key contributors to the proper stack operation. Uneven local utilization of the fuel is limiting the maximum practical utilization and decreasing electric efficiency of the stack. Additional loss of reactants through the sealing contributes to this effect. Flow distribution in the planar SOFC stack under electric load conditions and under high fuel utilization conditions is a complex process, affected by reactant gas physical characteristics, flow field geometry, dimensional characteristics of the cell package, stack manifolds design, flow direction in the inlet and outlet manifolds (U-flow, Z-flow), reactants flow field configuration (co-, cross-, counterflow), performance characteristics of the cell package and fabrication tolerances. In addition, flow distribution and pressure distribution in the fuel cell flow field and in the stack are coupled. The resulting pressure drop is contributing to the parasitic losses of the overall process. However, minimization of pressure drop in the flow field is limited by the resulting increase in the flow maldistribution.

Efforts to predict flow distribution of reactants in the fuel cell stack have been reported in literature using both analytical and computational fluid dynamics (CFD) methods. The electrochemical reactions under electric load conditions, chemical reactions in the gas phase and temperature distribution effects are often neglected due to computational complexity of the resulting problem.

In this work, the effect of fuel type was evaluated for a range of fuel streams derived from the process calculations using typical process configurations (steam reforming, fuel recycling loop) for the SOFC process design. Localized reactant flow conditions were derived from CFD calculations, accounting for both electrochemical reactions under load and chemical reactions in the gas phase. The results are also presented for the oxidant flow, which is several times higher then the corresponding fuel flow, in a typical range of oxidant utilizations. Systematic analysis of a range of effects and their relative importance on the flow distribution is presented. Operation of the stack under electric load conditions increases flow maldistribution of the fuel for the U-flow manifold configuration. The effect of the electric load on the oxidant flow is negligible for typical oxidant utilizations. The loss of reactants through the cell package sealing can increase flow maldistribution meaningfully. The CFD model calculations have been verified by the pressure drop measurements in the flow field.

Introduction

Flow distribution and pressure drop of reactants in the SOFC fuel cell stack are affecting both stack and system performance. Flow maldistribution of gas reactants in the fuel cell stack (and resulting uneven utilization of reactants) is one of the reasons for the performance loss in the cell scale-up process or even a stack failure at high electric load, high reactant utilization conditions. Efficient and uniform supply of reactants and removal of products have been studied previously. However, most of the modeling work involves numerous assumptions in order to reduce complexity of gas flow analysis in SOFC stack.

One of the earliest numerical macro-models of the planar fuel cell stack was introduced in 1994 by Costamagna et al. [1]. In this study, fuel cell stack was modelled as a system of manifolds connected to the parallel arrangement of the cell channels. Mathematical model was solved numerically and validated experimentally. Operation under ambient conditions with no electrochemical reactions was considered. A few years later Boersma and Sammes [2] proposed a model in which fuel cell stack was represented as a network of hydraulic resistances. This 2-dimensional model allows simulation of the gas flow and pressure distribution in the internally manifolded stack. Numerical results showed good convergence with analytical model.

In the literature, there are often presented analytical models of the pressure and flow distribution in the SOFC stack [3-4]. Such models can be used to simulate flow distribution in fuel cell stack, flow configuration of the inlet and outlet manifolds (U-flow, Z-flow), and dimensional characteristics of the cell package. Maharudrayya et al [4] compares analytical model results with 3-dimensional computational fluid dynamics (CFD) simulations. Analytical models typically assume no-load operating conditions.

CFD models allow detailed analysis of thermal, mass flow, and electrochemical processes in the stack. Van Herle et al. [5] present results of the non-isothermal CFD analysis of the SOFC stack with the emphasis placed on the issue of nickel anode reoxidation. Fluent CFD model of 60 planar cells stack (fabricated by Ceramatec Inc.) was developed at the Idaho National Laboratory [6]. The electrochemical add-on module allows investigation of coupled mass transport and electrochemical processes. Burt et al. [7] performed numerical investigation of cell-to-cell voltage variation. The fuel cell stack has been divided into computational domains with each cell treated as a separate process. The effect of radiation heat transfer on the cell performance was investigated by Tanaka [8]. Recently, numerous reviews of fuel cell modelling, approaches, techniques dealing with transport phenomena, electrochemical process and heat management within single cell and stack have been published [9], [10] [11].

Reaction kinetics and chemical equilibriums involved in the internal reforming of methane have been analysed by Sanchez et al. [12]. Nikooyeh et al. [13] investigated carbon formation in the process internal reforming of methane using 3-dimensional non-isothermal model. Ni et al. [14] developed mathematical model with both direct internal reforming of methane and water gas shift reaction included. The model has been validated using literature data. One-dimensional dynamic model of the internal reforming of methane, presented by Kang [15], offers decrease in computational time.

Internal reforming of methane in the anode supported SOFC button cell was investigated both experimentally and theoretically by Janardhanan and Deutschmann [16] with good agreement between data and simulation. The model was later extended to simulate temperature and current density distribution in the cell [17]. Klein et al. [18] investigated gradual internal reforming, showing that the cooling effect due to endothermal reforming reaction is eliminated when compared to direct internal reforming.

SOFC Stack Model

Stack - porous body.

The reactants supply system of the SOFC stack consists of air and fuel supply piping system, inlet and outlet manifolds and interconnects supplying reactants and collecting products from the reaction sites in the active area of the cell. Proper flow distribution of reactants contributes to optimal SOFC stack performance. However, a complete three-dimensional CFD approach to flow distribution calculations, including flow calculations in the interconnect channels, is computationally intensive and often requires simplifications.

Periodical and ordered geometry of the interconnect channels allows treatment of the SOFC stack as a porous body with porosity defined as a ratio of interconnect channels volume to stack volume in between manifolds:

$$\varphi = \frac{h \cdot w \cdot l \cdot n_{ch} \cdot n_c}{H \cdot W \cdot L}$$

where:

- φ – porosity
- h – channel height [m],
- H – manifold height [m],
- w – channel width [m]
- W – manifold width [m],
- l – channel length [m],
- L – distance between manifolds [m],
- n_{ch} – number of channels per cell,
- n_c – number of fuel cells in the stack.

Porous media are modelled by the addition of momentum source term to the standard fluid flow equations. The source term consists of viscous loss term (Darcy) and an inertial loss term where D_{ij} and C_{ij} are prescribed matrices [20].

$$S_i = -\left(\sum_{j=1}^{3} D_{ij} \mu v_j + \sum_{j=1}^{3} C_{ij} \frac{1}{2} \rho v_{mag} v_j \right)$$

In the case of laminar flow through the porous stack body, only the viscous loss term is applicable. As the first step, pressure drop in a single channel is calculated based on the fluid properties, channel dimensions and flow. Analytical equations are used in calculations. Pressure drop, Δp, in a single channel of interconnect is expressed as:

$$\Delta p = -S_i \Delta n$$

were Δn represents thickness. From the above equations resistance factor is calculated as:

$$D_{ij} = \frac{\frac{\Delta p}{v}}{\mu l \varphi}$$

where:

- v velocity [m/s]
- μ viscosity [N*s/m2]
- l length of channel [m]
- φ porosity

Since porous body, representing electrochemically active part of the SOFC stack, is impermeable in directions other than flow direction in gas channels, father simplifications of the CFD stack model are possible, including two-dimensional CFD model approach. In two-dimensional (2D) model, impermeable direction is represented by a viscous resistance coefficient, several orders of magnitude higher than the permeable direction.

Comparison between 3D & 2D numerical model

In the first step, two-dimensional and three-dimensional CFD models of the SOFC stack have been compared. Both models represented 57 cells SOFC stack with 50 mm square cells, 10 mm wide manifolds and interconnects with 0.8x0.8x50 mm gas channels. The electrochemical model was turned off for the model comparison. The results of static pressure distribution calculations for 2D and 3D stack models are shown in Figure 1. Since the differences between models are minor, 2D model has been selected for calculations

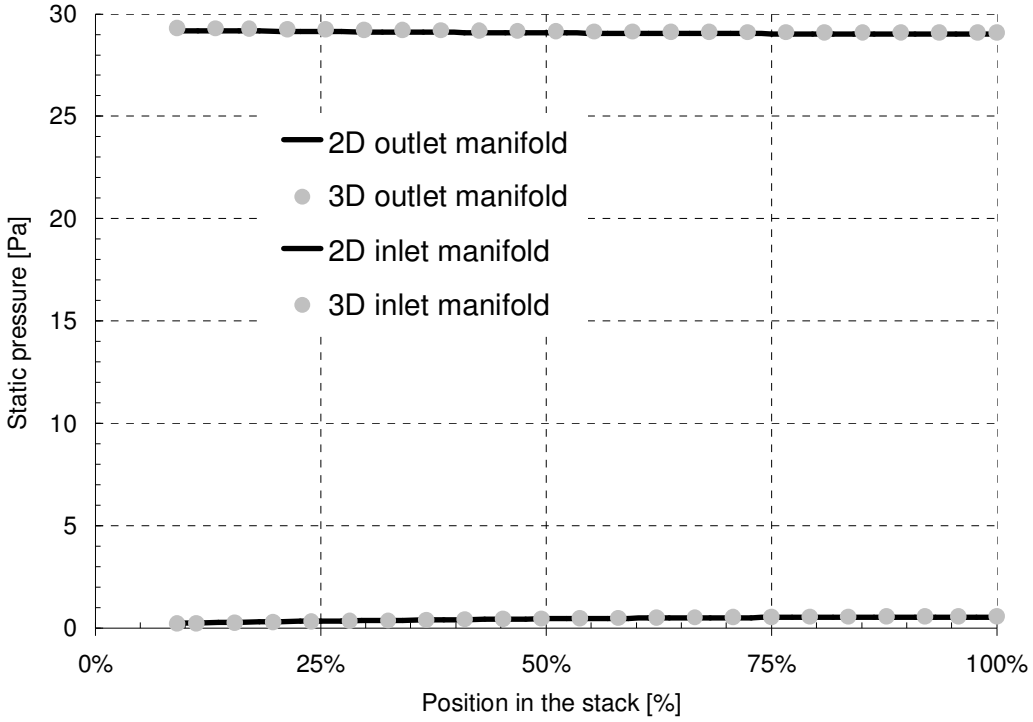

Figure 1. Comparison of static pressure distribution in the stack manifolds for two-dimensional and three-dimensional CFD stack flow distribution models, along the stack centreline (0% - bottom of the stack, 100% top of the stack).

Electrochemical model

In the present study, mass transport phenomena in the SOFC fuel cell stack are coupled with chemical and electrochemical reactions, including water-shift reaction, internal reforming of methane, anodic and cathodic electrochemical reactions. The resulting model was implemented in the CFD Fluent® software and used to predict 1.2 kW SOFC stack performance. The load performance was approximated by the equation:

$$i = \frac{E - V}{R_{ir} + R_a + R_c}$$

where:

i – current density [A/m2],

E – Nernst voltage [V],
V – cell voltage [V],
R_{ir}, R_a, R_c – internal resistance, anode resistance and cathode resistance, respectively [Ohm m^2]

The *ASR* (Area Specific Resistance) data for a single cell, for a range of temperatures and gas compositions, were fitted to semi-empirical equation and used to simulate single cell local performance in the CFD calculations. The assumed average current density of the stack was specified as the input value to calculate cell voltages iteratively.
The production and consumption of species due to electrochemical reactions was described as:

$$S_{electr,H2} = -\frac{i \cdot M_{H2}}{2 \cdot F} \;\; ; \; S_{electr,O2} = -\frac{i \cdot M_{O2}}{4 \cdot F} \;\; ; \; S_{electr,H2O} = \frac{i \cdot M_{H2O}}{2 \cdot F}$$

where:
i – local current density [A/m^2]
M_i – molar mass [kg/kmol],
F – Faraday constant [C/kmol].

Internal reforming of methane

High temperature fuel cells in contrast to low temperature fuel cells can convert both hydrogen and carbon monoxide to electricity. Moreover, high temperature fuel cell can be fed with methane containing fuel. Methane can be converted to H_2 and CO in a steam reforming endothermic reaction at the SOFC anode:

$$CH_4 + H_2O \rightarrow 3H_2 + CO$$

Steam reforming process is associated with a water-shift reaction:

$$CO + H_2O \rightarrow CO_2 + H_2$$

Both steam reforming of methane and water-shift reactions are included in present model of the SOFC stack. Water-shift reaction is assumed to reach equilibrium locally at any location in the stack:

$$K_{eq,shift} = \frac{p_{H2} \cdot p_{CO2}}{p_{CO} \cdot p_{H2O}} = \frac{N_{H2} \cdot N_{CO2}}{N_{CO} \cdot N_{H2O}}$$

where N [kmol/s] denotes local molar flux of selected species. Additionally, shift equilibrium constant is calculated as a function of operating temperature from the equation [21]:

$$\ln(K_{eq,shift}) = \frac{5693.5}{T} + 1.077\ln(T) + 5.44 \cdot 10^{-4} \cdot T - 1.125 \cdot 10^{-7} \cdot T^2 - \frac{49170}{T^2} - 13.148$$

where T [K] denotes operating temperature of the fuel cell.

For the internal reforming of methane, finite rate of reforming is assumed in the model, with the rate constants taken from Achenbach [22]:

$$S_{ref,CH4} = \gamma \cdot p_{CH4}^m \cdot p_{H2O}^n \cdot \exp\left(-\frac{E_a}{R \cdot T}\right)$$

where:
γ - preexponential factor, γ = 4.274 [kmol/s-m^2-atm]
p_{CH4}, p_{H2O} – partial pressure of methane and water, respectively [atm],

m – exponential parameter, m=1
n – exponential parameter, n=0
E_a – activation energy of methane reforming process, $E_a = 8.2 \cdot 10^{-7}$[J/kmol].

According to Achenbach [22], changing the H_2O/CH_4 ratio from 2.6 to 8 has no dramatic effect on reforming process. Finally, the rates of formation for individual species of the fuel mixture, including water-shift reaction, finite reforming rate and electrochemical reactions can be presented as:

$$S_{CH4} = -S_{ref,CH4}$$
$$S_{CO} = S_{ref,CH4} - S_{shift}$$
$$S_{H2O} = -S_{ref,CH4} - S_{shift} + S_{electr,H2O}$$
$$S_{H2} = 3 \cdot S_{ref,CH4} + S_{shift} - S_{electr,H2}$$
$$S_{CO2} = S_{shift}$$

Modelling and simulations

Flow geometry.

The planar SOFC stack used in the CFD simulation is illustrated in Figure 2. The stack consists of identical 50x50 mm cells with 8 mm wide manifolds and square 8 mm wide reactant distribution channels. CFD simulations were performed for two types of manifold configurations: U – flow and Z – flow.

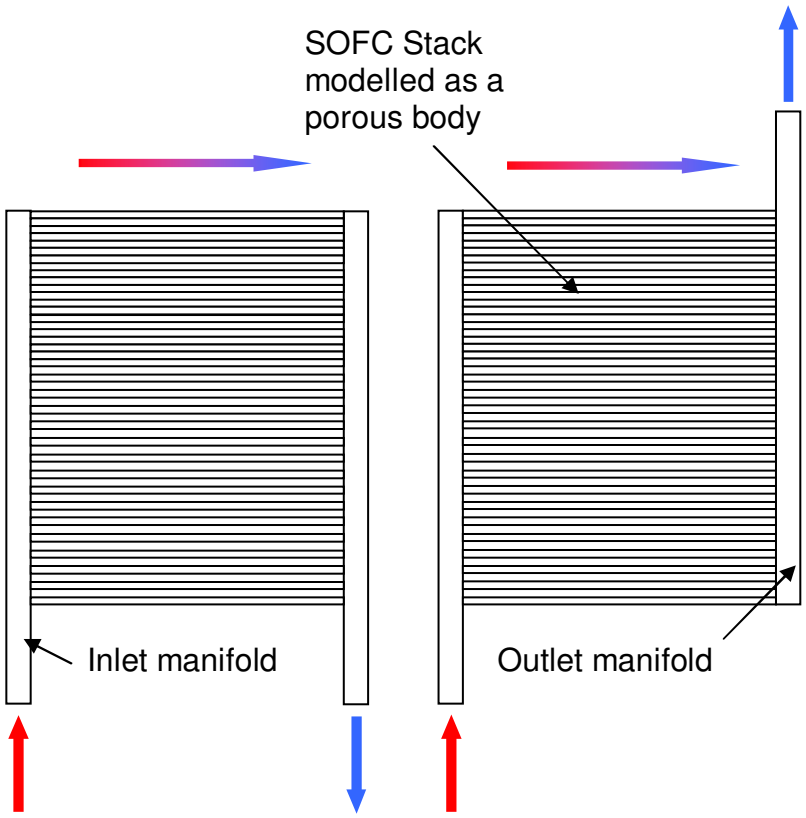

Figure 2. Model representation of the stack manifolding and cell channels geometry

Numerical model validation

The 2-dimensional CFD model was verified using experimental setup for the cathode pressure drop measurements. For the oxidant flow rates corresponding to a range of oxidant utilizations from 15% to 50%, a number of flow related characteristics have been measured, including inlet and outlet oxidant flow rates, inlet fuel flow rate, differential pressure across cathode, differential pressure across anode and absolute pressure at the cathode inlet. Some of the results are shown in Figure 3 together with the corresponding model simulation results.

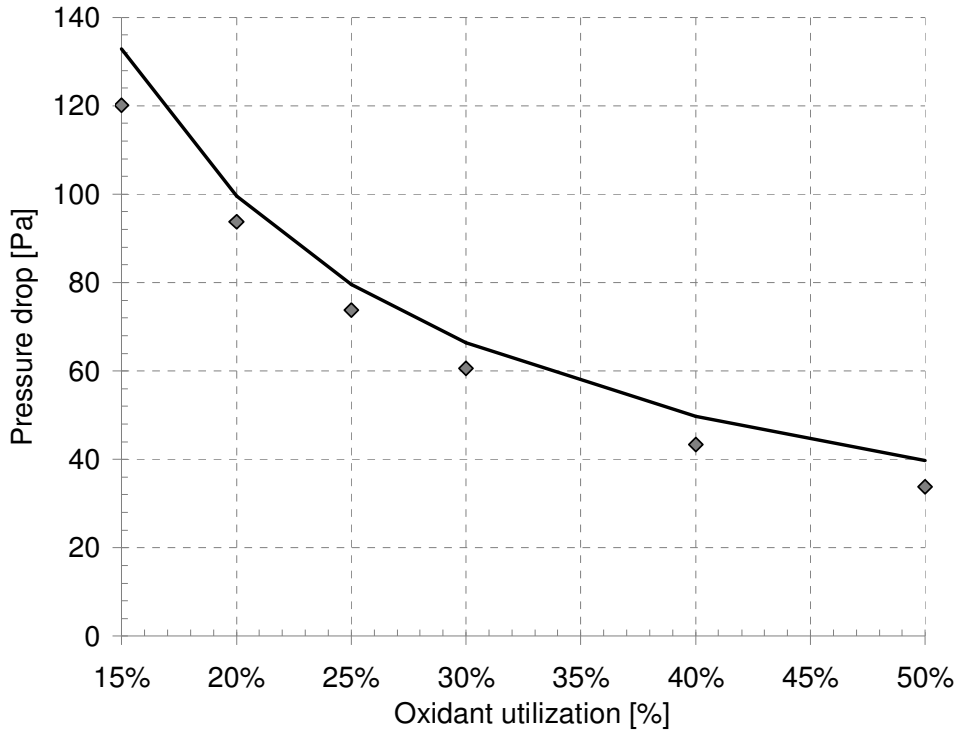

Figure 3. Comparison of pressure drop [Pa] across the cathode side of the SOFC cell for a range of oxidant utilizations [%] corresponding to current density of 5000 [A/m^2] at 800 [C] average cell temperature (— - simulation results, ♦ - measurements);

Optimization of reactant distribution channels

Flow distribution of oxidant and fuel in the stack with internal manifolds depends mainly on the dimensional factors. The ratio of pressure drop in the manifolds to pressure drop in the interconnect channels is a qualitative measure of the flow maldistribution.

The effect of pressure drop increase in the interconnect channels with the increase of the channel height is shown in Figure 4. Simultaneously, homogeneity of fuel and air flow improves significantly. The maximum and minimum flow deviations are calculated along the stack centreline, relative to the average flow in the cell:

$$Flow\_Maldistribution = \frac{Maximum\_Flow - Minimum\_Flow}{Average\_Flow}$$

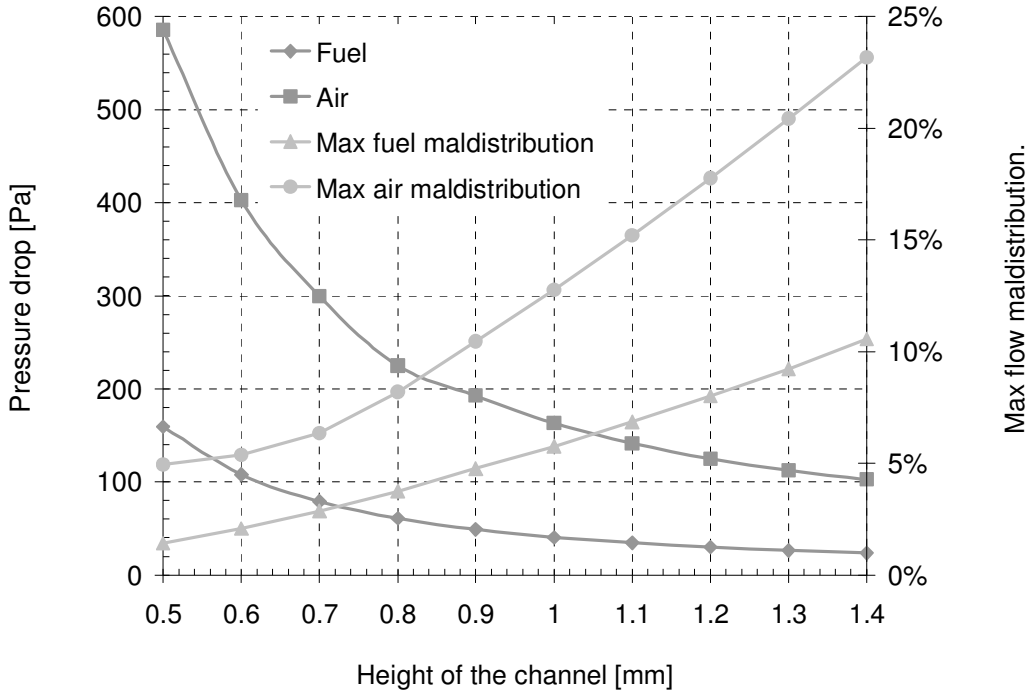

Figure 4. Pressure drop and maximum flow maldistribution as a function of interconnect channel height (fuel utilization – 60%, oxidant utilization - 20%, average stack current density 5000 [A/m2], interconnect channel width – 8 [mm])

Manifold configuration and fuel composition effects

Two-dimensional CFD model of the SOFC stack was applied to simulate flow distribution under electric load conditions for the selected fuels. Typical flow arrangements of the inlet and outlet gas supply manifolds, U-flow and Z-flow (Figure 2), have also been evaluated. The results of the flow maldistribution for the 48.5%H_2/48.5N_2/3%H_2O fuel mixture (Figure 5), partially reformed natural gas (Figure 6) and completely reformed natural gas (Figure 7), for the stack operating at both open cell voltage conditions (OCV) and electric load corresponding to 8000A/m^2, are presented for both U-flow and Z-flow configurations.

In each case, fuel flow distribution in the SOFC stack operating under electric load condition is more non-uniform when compared to open cell voltage conditions. The differences are more pronounced for the partially and completely reformed natural gas. This can be explained by the differences in the fuel flow rates, fuel viscosity changes due to anodic reactions under electric load conditions (Table 1) and corresponding pressure drop differences. In the case of partial steam reforming of methane, flow maldistribution in the U-flow configuration increases from 3.0% at OCV conditions to 4.4% under electric load conditions.

The Z-flow configuration of manifolds generates lower flow maldistribution than the U-flow configuration. It is particularly visible for the fuels generated in partial and complete steam reforming of natural gas (Figures 6-7). In the U-flow configuration, more of the fuel is directed to fuel cells at the bottom of the stack while fuel supply to the top of the stack is depleted. The reversing of the fuel supply is typical for the Z-flow configuration where more of the fuel is supplied to the top of the stack.

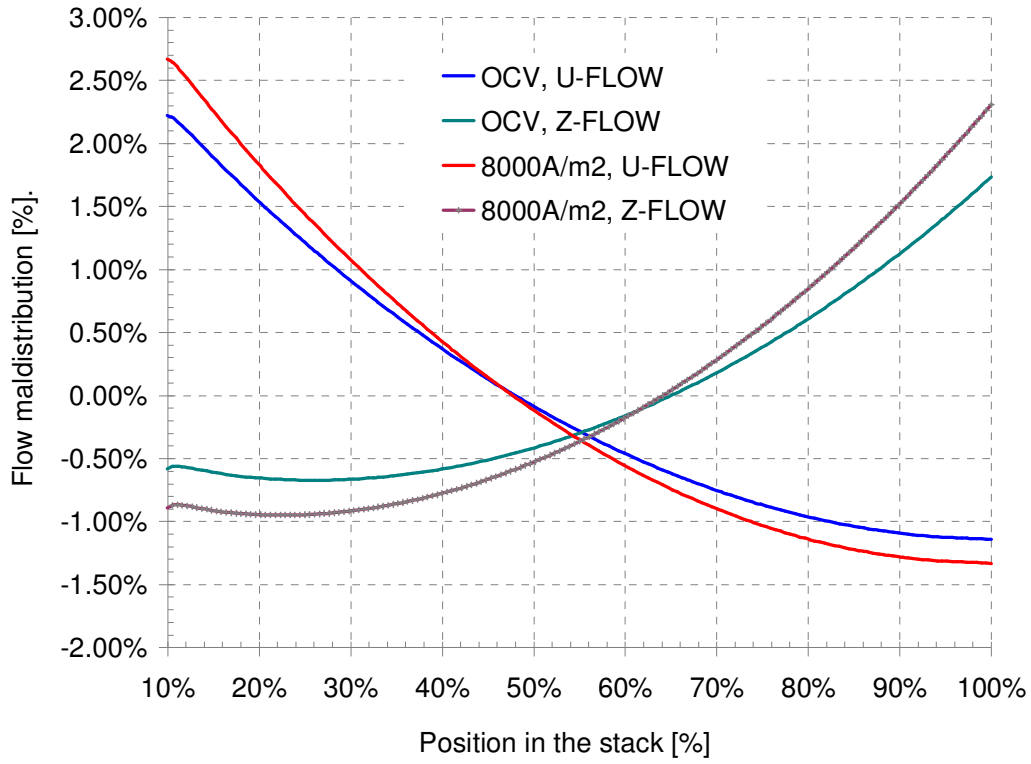

Figure 5. Flow maldistribution of the fuel along the stack centreline (0% - bottom of the stack, 100% top of the stack) for the 48.5%H_2 / 48.5N_2 / 3%H_2O fuel mixture.

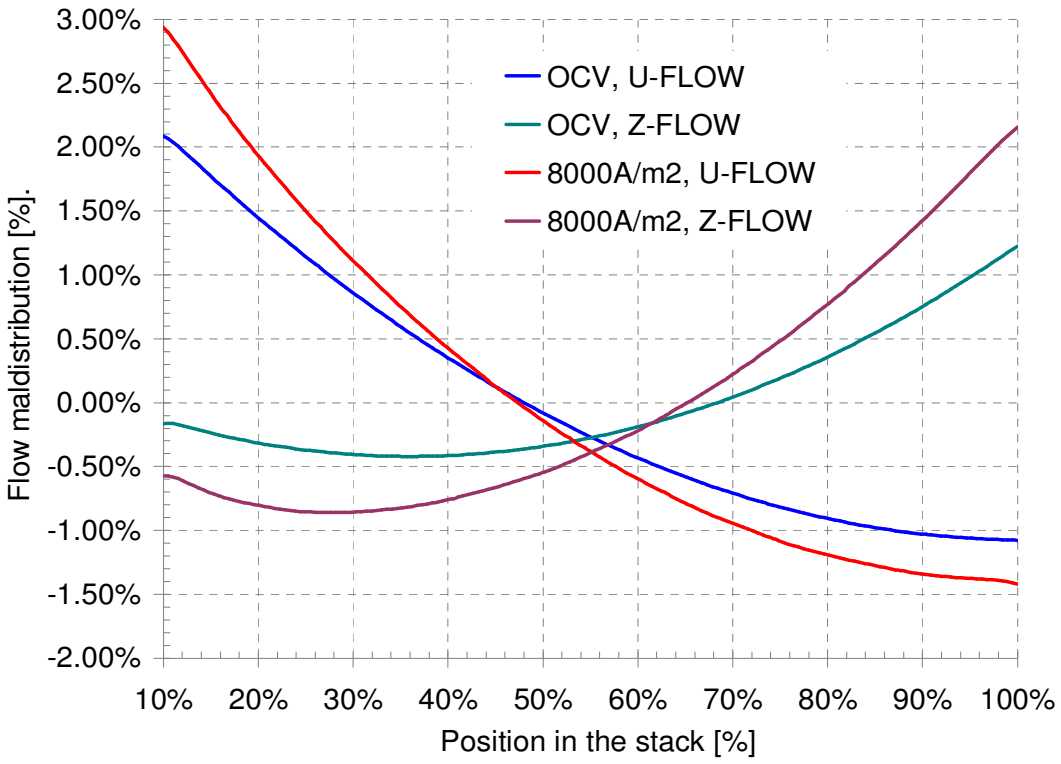

Figure 6. Flow maldistribution of the fuel along the stack centreline (0% - bottom of the stack, 100% top of the stack) for the partially reformed natural gas (NG:H_2O=2.5:1).

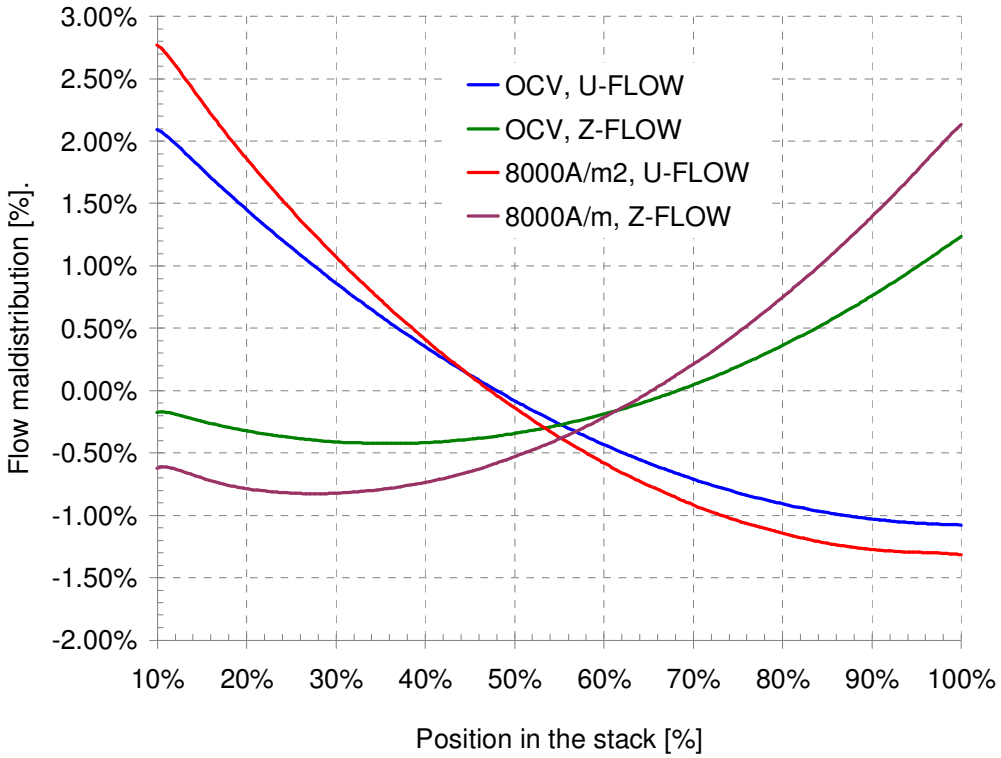

Figure 7. Flow maldistribution of the fuel along the stack centreline (0% - bottom of the stack, 100% top of the stack) for the completely reformed natural gas (NG:H_2O=2.5:1).

Pressure drop across the fuel channels changes with the fuel utilization as shown in Figure 8 for all three fuel types analysed (at the average current density of 5000A/m^2). Much higher pressure drop for the 48.5%H_2/48.5%N_2/3%H_2O fuel mixture is partially explained by the higher dynamic viscosity of this fuel at the fuel inlet to the stack (Table 1)

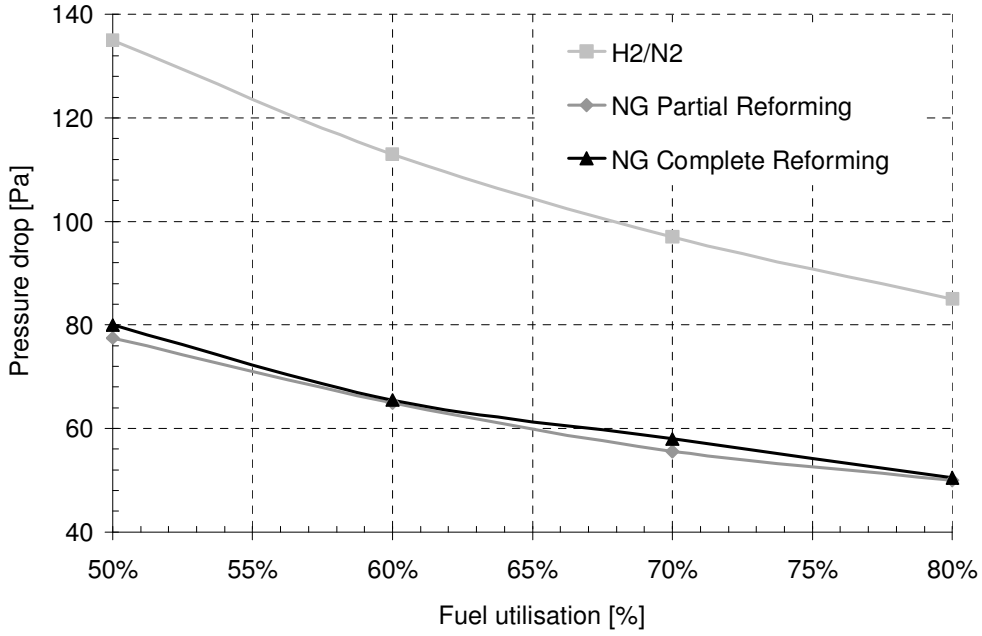

Figure 8. Pressure drop for the fuel side of the stack as a function of fuel utilization (NG-natural gas)

Table 1. Dynamic viscosity of the selected fuel compositions at the stack inlet and stack outlet locations.

	Inlet Mixture Viscosity [kg/m^2 s]	Outlet Mixture Viscosity [kg/m^2 s]			
		FU 50%	FU 60%	FU 70%	FU 80%
48.5%H_2/%48.5N_2 balance H_2O	4.165E-05	4.270E-05	4.282E-05	4.293E-05	4.301E-05
NG - Partial Reforming	3.468E-05	3.961E-05	4.030E-05	4.096E-05	4.151E-05
NG - Complete Reforming	3.421E-05	3.961E-05	4.033E-05	4.096E-05	4.151E-05

On the other hand, both dynamic viscosity and flow rates are very similar for the partially and completely reformed natural gas. The molar fraction changes along the interconnect fuel channels are shown in Figure 9 ($H_2/N_2/H_2O$ mixture) and Figure 10 (partially reformed natural gas) for the 80% fuel utilization at 5000A/m^2 electric load. In the case of partially reformed natural gas, methane present at the fuel inlet at 13 mol % is completely converted to H_2/CO at 1/3 of the fuel channel length.

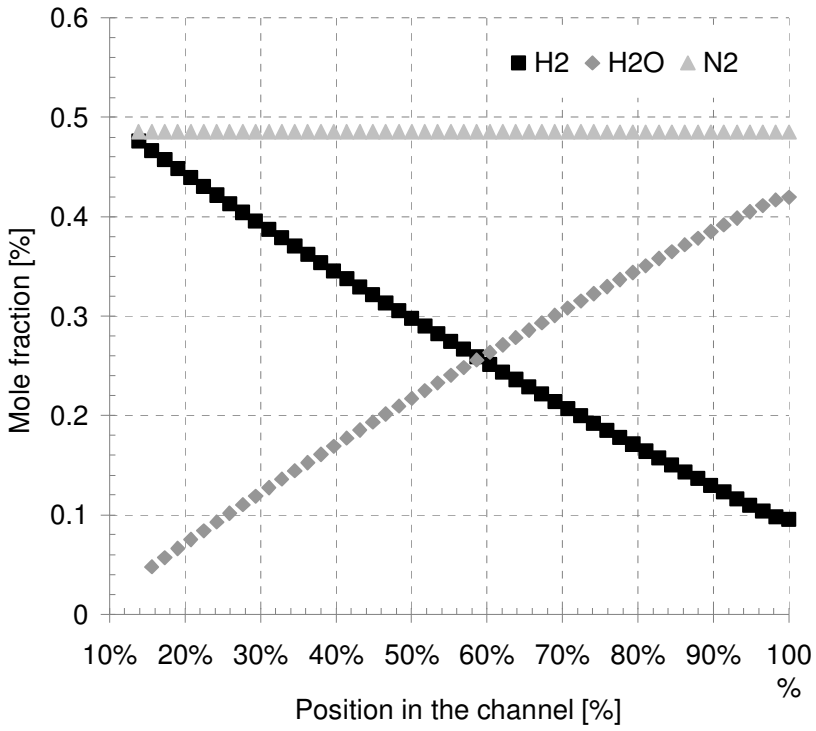

Figure 9. Fuel composition along the interconnect channel for the 48.5%H_2 / 48.5N_2 / 3%H_2O fuel mixture (0% - inlet of the channel, 100% outlet of the channel).

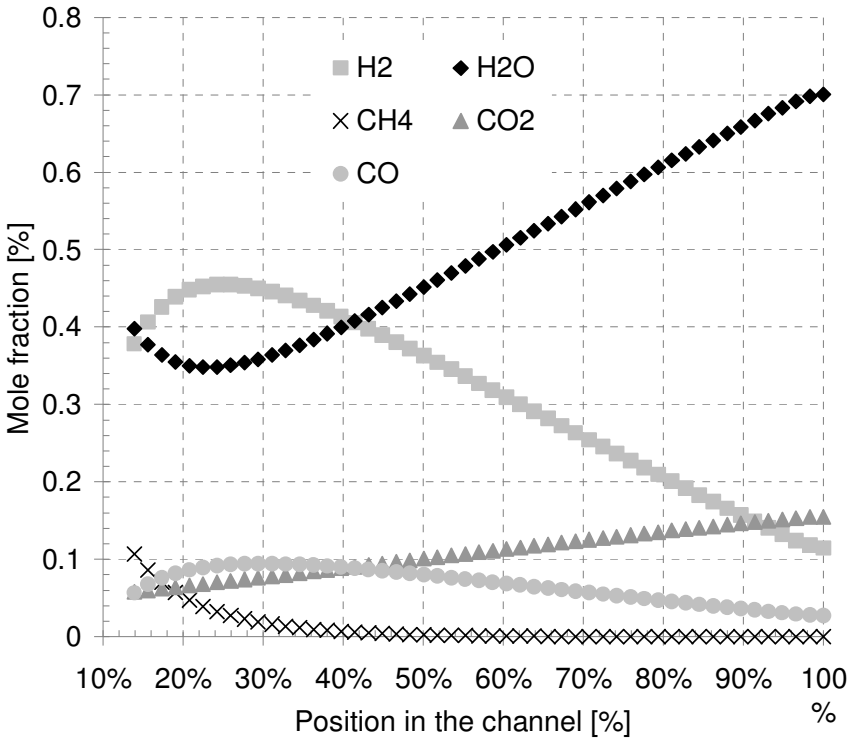

Figure 10. Fuel composition along the interconnect channel for the partially reformed natural gas (0% - inlet of the channel, 100% outlet of the channel).

Summary

Two-dimensional CFD flow distribution model, described in this paper, has been developed to simulate flow distribution and pressure distribution in the SOFC stack under electric load conditions in the Z-flow and U-flow manifold configurations. Both water-shift equilibrium reaction and finite rate of methane reforming are included in the model to compute local gas compositions. In addition, effects associated with the reactant loss through the seals are incorporated in the model. The interconnect flow field was optimized at first in order to optimize pressure drop in the cell and flow distribution in the stack. The results of two-dimensional model were compared with the three-dimensional flow distribution model. There are only minor differences in the results computed using both models. The CFD model was verified using pressure drop data across the cathode side of the cell. Flow maldistribution in the stack was calculated for several fuels. The Z-flow configuration of manifolds generates lower flow maldistribution than the U-flow configuration. In the U-flow configuration, more of the fuel is directed to fuel cells at the bottom of the stack while fuel supply to the top of the stack is depleted.

Acknowledgements

Financial support from the European Regional Development Fund and Ministry of Science and Education under the project no. UDA-POIG.01.01.02-00-016/08-00 and European Commission under the project no. 231058 is gratefully acknowledged.

References

[1] P. Costamagna, E. Arato, E. Achenbach, U. Reus “Fluid dynamic study of fuel cell devices: simulation and experimental validation.” Journal of Power Sources 52 (1994) 243-249.

[2] R.J. Boersma, N.M. Sammes “Distribution of gas flow in internally manifolded solid oxide fuel-cell stacks.” Journal of Power Sources 66 (1997) 41-45

[3] Robert J. Kee, Pavan Korada, Kevin Walters, Mark Pavol, “A generalized model of the flow distribution in channel networks of planar fuel cells.” Journal of Power Sources (2002) 148-159.

[4] S. Maharudrayya, S. Jayanti, A.P. Deshpande, “Pressure drop and flow distribution in multiple parallel-channel configurations used in proton-exchange membranes fuel cell stack.” Journal of Power Sources 157 (2006) 358-367.

[5] J. Van Herle, D. Larrain, N. Autissier, Z. Wuillemin, M. Molinellis, D. Favrat, “Modeling and experimental validation of solid oxide fuel cell materials and stacks.” Journal of the European Ceramic Society 25 (2005) 2627-2632.

[6] Gant Hawkes, James O’Brien, Carl Stoots, Brian Hawkes, “3D CFD Model of a Multi-Cell High Temperature Electrolysis Stack.” 2007 AIChE Annual Meeting.

[7] A.C. Burt, I.B. Celik, R.S. Gemmen, A.V. Smirnov, “A numerical study of cell-to-cell variations in SOFC stack.”, Journal of Power Sources 126 (2004) 76-87.

[8] T. Tanaka, Y. Inui, A. Urata, T. Kanno, “Three dimensional analysis of planar solid oxide fuel cell stack considering radiation.” Energy Conversion and Management 48 (2007) 1491-1498.

[9] Luca Andreassi, Giampiero Rubeo, Stefano Ubertini, Piero Lunghi, Roberto Bove, “Experimental and numerical analysis of a radial flow solid oxide fuel cell.” International Journal of Hydrogen Energy 32 (2007) 4559-4574.

[10] Roberto Bove, Stefano Ubertini, “Modelling solid oxide fuel cell operation: Approaches, techniques and results.” Journal of Power Sources 159 (2006) 543-559.

[11] Sadik Kakac, Anchasa Pramuanjaroenkij, Xiang Yang Zbou, “A review on numerical modeling of solid oxide fuel cells.” International Journal of Hydrogen Energy 32 (2007) 761-786.

[12] D. Sanchez, R. Chacartegui, A. Munoz, T. Sanchez, “On the effect of methane internal reforming modelling in solid oxide fuel cells.” International Journal of Hydrogen Energy 33 (2008) 1834-1844.

[13] Kasra Nikooyeh, Ayodeji, A. Jeje, Josephine M. Hill, “3D modelling of anode-supported planar SOFC with internal reforming of methane.” Journal of Power Sources 171 (2007) 601-609.

[14] Meng Ni, Dennis Y.C. Leung, Michael, K.H. Leung, “Electrochemical modelling and parametric study of methane fed solid oxide fuel cells.” Energy Conversion and Management 50 (2009) 268-278.

[15] Ying-Wei Kang, Jun Li, Guang-Yi Cao, Heng-Yong Tu, Jian Li, Jie Yang, “A reduced 1D dynamic model of a planar direct internal reforming solid oxide fuel cell for system research.” Journal of Power Sources (2009) 170-176.

[16] Vinod M. Janardhanan, Olaf Deutschmann, “CFD analysis of a solid oxide fuel cell with internal reforming: Coupled interactions of transport, heterogeneous catalysis and electrochemical processes.” Journal of Power Sources 162 (2006) 1192-1202.

[17] Vinod M. Janardhanan, Olaf Deutschmann, “Numerical study of mass and heat transport in solid-oxide fuel cells running on humidified methane.” Chemical Engineering Science 62 (2007) 5473-5486.

[18] J.M. Klein, Y. Bultel, S. Georges, M. Pons, “Modeling of a SOFC fuelled by methane: From direct internal reforming to gradual internal reforming.” Chemical Engineering Science (2007) 1636-1649.
[19] Qiusheng Wang, Lijun Li, Cheng Wang, “Numerical study of thermoelectric characteristics of planar solid oxide fuel cell with direct reforming of methane.” Journal of Power Sources 186 (2009) 399-407.
[20] www.fluent.com
[21] Y. Choi, H.G. Stenger, “Water gas shift reaction kinetics and reactor modelling for fuel cell grade hydrogen.” Journal of Power Sources 124 (2003) 432-439.
[22] E. Achenbach, E. Riensche, “Methane/Steam reforming kinetics for solid oxide fuel cells.” Journal of Power Sources 52 (1994) 283-288.